AAPS PharmSciTech, Vol. 14, No. 2, June 2013 (© 2013)
DOI: 10.1208/s12249-013-9963-z

Research Article

Binding Interactions of Naringenin and Naringin with Calf Thymus DNA and the Role of β-Cyclodextrin in the Binding

Sameena Yousuf[1] and Israel V. Muthu Vijayan Enoch[1,2]

Received 7 August 2012; accepted 25 March 2013; published online 27 April 2013

Abstract. The interaction of naringenin (Nar) and its neohesperidoside, naringin (Narn), with calf thymus deoxyribonucleic acid (ctDNA) in the absence and the presence of β-cyclodextrin (β-CD) was investigated. The interaction of Nar and Narn with β-CD/ctDNA was analyzed by using absorption, fluorescence, and molecular modeling techniques. Docking studies showed the existence of hydrogen bonding, electrostatic and phobic interaction of Nar and Narn with β-CD/DNA. 1:2 stoichiometric inclusion complexes were observed for Nar and Narn with β-CD. With the addition of ctDNA, Nar and Narn resulted into the fluorescence quenching phenomenon in the aqueous solution and β-CD solution. The binding constant K_b and the number of binding sites were found to be different for Nar and Narn bindings with DNA in aqueous and β-CD solution. The difference is attributed to the structural difference between Nar and Narn with neohesperidoside moiety present in Narn.

KEY WORDS: calf thymus DNA; β-cyclodextrin; naringenin; naringin.

INTRODUCTION

The physicochemical analysis of the binding of small molecules with macromolecules like nucleic acids and proteins plays a vital role to explore the application of the molecule in the field of drug delivery. The interaction between various small molecules and DNA is an important fundamental issue in life science that is related to the replication and transcription of DNA *in vivo*, mutation of genes and related variations of species in character, action mechanism of some DNA-targeted drugs, origin of some disease, and action mechanism of some synthetic chemical nucleases and so on (1). Significant progress has been made over the past few years in studies of drug–DNA interactions. Structure-based design strategies have yielded new DNA-binding agents with clinical promise (2). Various physicochemical methods have been utilized to find such interactions (3–5). The absorption and fluorescence techniques are the widely used tools due to their good repeatability and high sensitivity (6,7). Fluorescence properties are generally sensitive to changes in the physical and chemical environment and can be used to characterize the rigid dynamics of macromolecules to which they are attached (8). Modern method of drug designing uses computational chemistry to study about the drugs and related biological active molecules. Structure-based and ligand-based drug designing softwares have potential applications in the pharmaceutical field to design novel drugs. In case of ligand-based drug designing, software is mainly used for docking the ligand with target drug molecules. Schrodinger software provides accurate, reliable, and high-performance computational technology and provides facilities to solve problems in life science research. It was used for molecular modeling and well suited for drug designing both structure-based and ligand-based methods. Glide offers a complete solution for ligand receptor docking with speed and accuracy (9).

Naringenin and naringin (naringenin-7-*O*-neohesperidoside) are bioactive flavonoids which are present in substantial amounts in plants (10,11). Naringin is one of the reasons for the overall antioxidant activity of citrus fruit (12). Grapefruit has total flavanone content of 27 mg/100 g as aglycones and a distinct flavanone profile, dominated by naringin (13). It blocks the lipopolysaccharide-induced transcriptional activity of tumor necrosis factor alpha (14). Naringin is metabolized to the flavanone, naringenin in humans. Naringenin possesses anti-inflammatory, anti-carcinogenic, and anti-tumor effects (15). Naringenin has recently been shown to exert hypolipidemic and hypocholesterolemic effects, which are particularly important for protecting against chronic diseases (16). Metabolism and excretion studies of oral administered naringin in rats and dogs showed that about 21% of administered naringin was recovered in rat excreta in the form of naringin, total naringenin, and 4-hydroxy phenyl propionic acid, and about 60% was recovered in dog excreta (17). The study on the fate of naringin in humans suggests that cleavage of the sugar moiety, presumably by intestinal bacteria, is the first step of naringin metabolism. Here, naringenin formation is thought to be the crucial step in determination of bioavailability of the compound, which undergoes rapid glucuronidation (18). Since naringin and naringenin play a vital role in the metabolism of humans, it is necessary to enhance its aqueous solubility/bio availability by studying the comparison on naringin/naringenin interaction with β-cyclodextrin (β-CD)/DNA.

[1] Department of Chemistry, Karunya University, Coimbatore 641 114, India.
[2] To whom correspondence should be addressed. (e-mail: drisraelenoch@gmail.com)

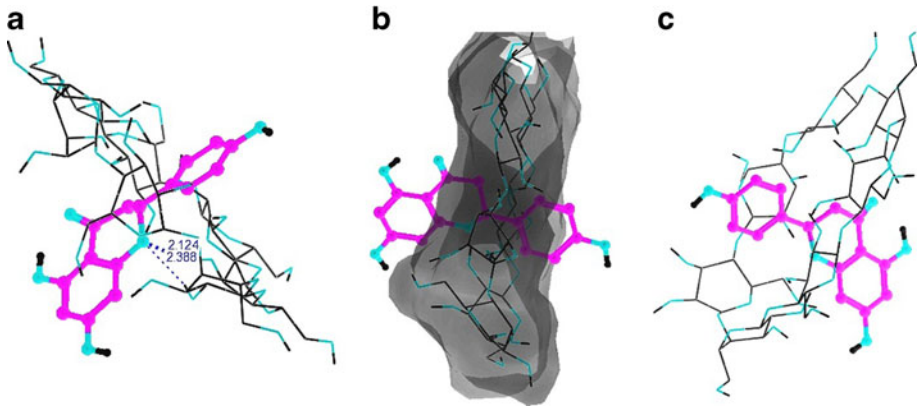

Fig. 1. Docking poses of naringenin with β-cyclodextrin. **a** Hydrogen interaction. **b** Phobic interaction. **c** Electrostatic interaction

CDs are cyclic D-glucopyranoses bonded through alpha-1, 4-glycosidic linkages. Some major cyclodextrins (α-, β-, and γ-CDs) are produced from starch by bacterial cyclodextrin glycosyltransferase (19,20). CDs, which are bucket-shaped cyclic oligosaccharides, allow molecules of appropriate size to be incorporated inside their hydrophobic inner cavity for the slow release of the molecules, mainly in the field of drug delivery. In addition, the hydrophilic exterior nature of CDs helps to increase the solubility of the small molecules which act as drugs (21). There are approximately 30 different pharmaceutical products worldwide containing drug/cyclodextrin complexes on the market (22). In studying the interaction of small molecules with DNA, CDs are mainly used for three purposes viz., (a) to increase the solubility of the drug molecules, (b) to increase the fluorescence intensity of the drug molecules by forming inclusion complexes, and (c) to tune the molecule for the selective interaction of a specific moiety with DNA backbone by incorporating the undesired hydrophobic moiety with β-CD. β-CD has been used as the host medium to reveal the specific interacting site of the small molecule with DNA (1,23). The present work deals with the analysis on the interaction of Nar and Narn with ctDNA in the absence and the presence of β-CD medium. The effect of neohesperidoside group on the stoichiometry and the binding of Nar and Narn with β-CD/ctDNA were investigated. The interaction between Nar/Narn and β-CD/DNA was analyzed by molecular docking analysis.

MATERIAL AND METHOD

Material

Calf thymus DNA (Genei, India) was used as such without further purification. The purity of ctDNA was determined

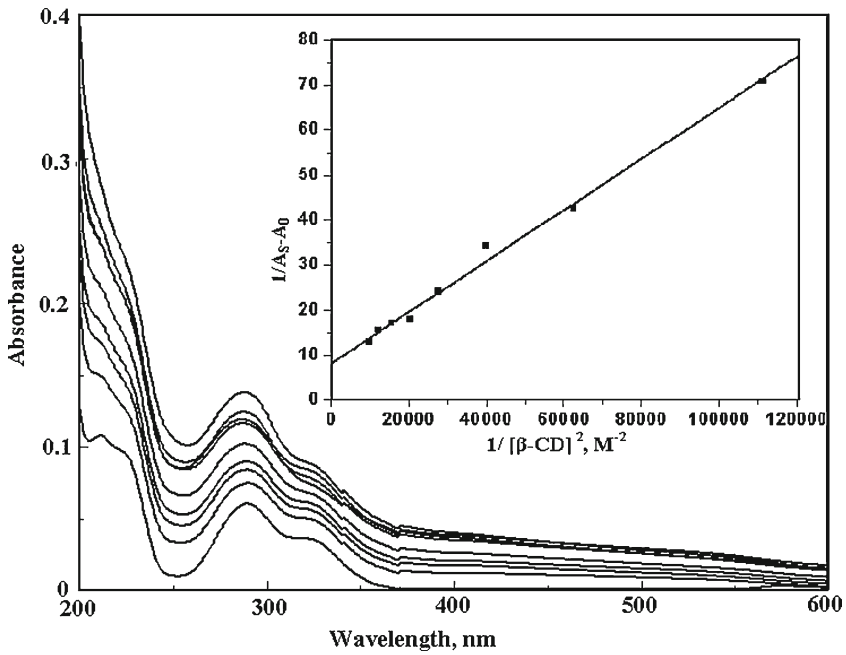

Fig. 2. Absorption spectra of naringenin in the presence of various concentrations of β-cyclodextrin. *Inset* The plot of $1/A_s–A_0$ against $1/[\beta\text{-CD}]^2$ for the interaction of naringenin in the presence of various concentrations of β-CD

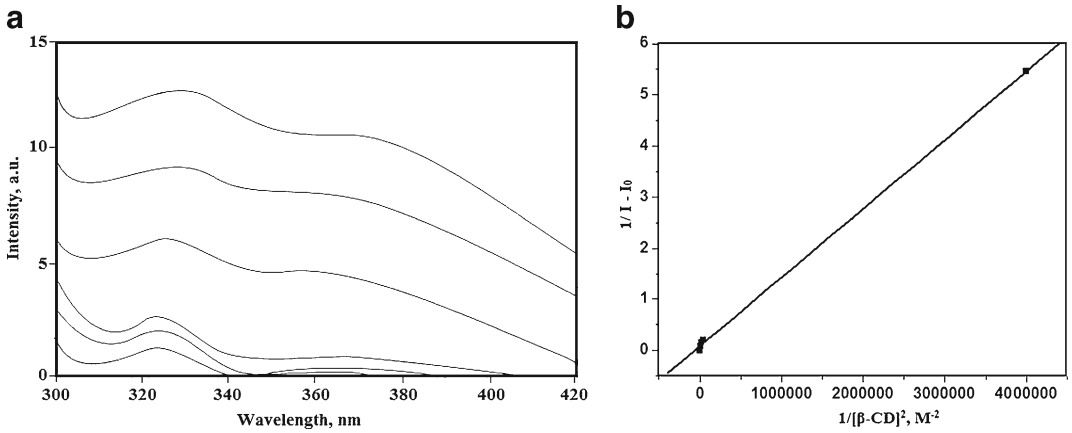

Fig. 3. **a** Fluorescence spectra of naringenin in the presence of various concentrations of β-cyclodextrin. **b** The plot of $1/I-I_0$ against $1/[\beta\text{-CD}]^2$ for the interaction of naringenin in the presence of various concentrations of β-CD

from optical measurements ($A_{260}/A_{280}>1.8$, where A represents absorbance). ctDNA was dissolved in 50 mmol of NaCl prior to use to obtain the concentration of 2.27×10^{-4} mol/L (per nucleotide phosphate) which was calculated using the molar extinction coefficient of 6,600 L (mol cm) at 260 nm. Naringenin and naringin were obtained from Sigma, India. β-CD was obtained from Hi-Media, India. Ten millimolars (pH, 3.5) acetate buffer solution was used to control the pH value. Doubly distilled water was used throughout, and the solutions were stored at 0°C to 4°C. All the experiments were carried out at an ambient temperature of 25±2°C.

Procedure

One milliliter of 10 mM acetate buffer was transferred into microtubes. Aliquots of Nar/Narn and β-CD/ctDNA from their stock solution were added and made up to the required concentration by diluting with double distilled water. The solution was shaken well after all the additives were added, and the measurements of absorption and fluorescence were made against the appropriate blank solution. Both the excitation and the emission band width were set up at 4 nm. Absorption measurements were performed with a UV–visible spectrophotometer (V-630, Jasco, UK) using a 1-cm path-length cell. Fluorescence spectra were recorded on a spectrofluorimeter (Jasco FP 750, UK) equipped with a 150-W Xenon lamp. Molecular modeling studies were carried out using Schrodinger with the software, glide, version 5.5 to determine the interaction of Nar and Narn with DNA/β-CD (24). The structure of ctDNA duplex 5′-d $(CCATTAATGG)_2$-3′ was built and optimized (25). The docking tool was applied to generate Nar–β-CD, Narn–β-CD, Nar–DNA, and Narn–DNA

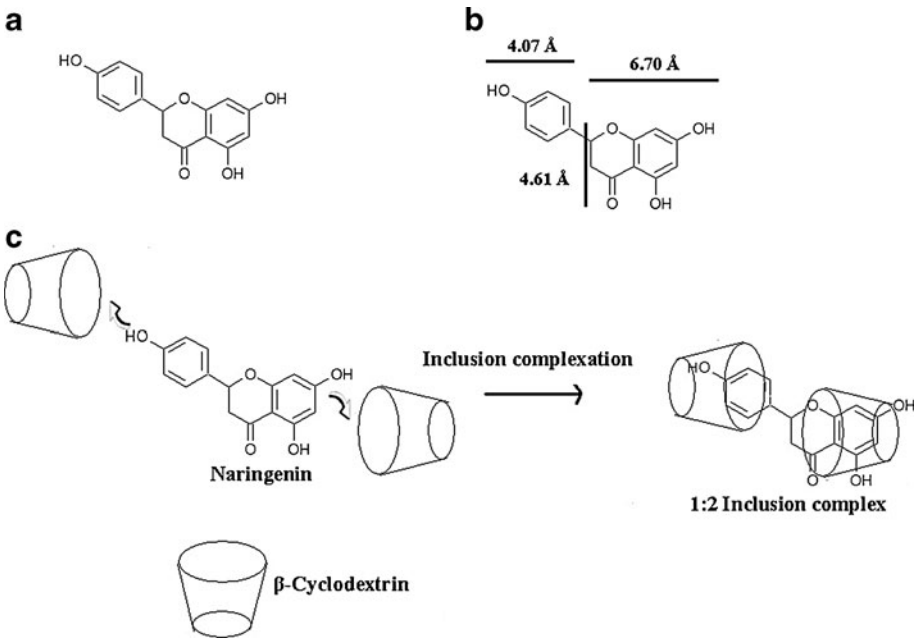

Fig. 4. **a** The molecular structure of naringenin. **b** The calculated length and width of naringenin. **c** Schematic diagrams of the 1:2 inclusion complexation of naringenin with β-CD

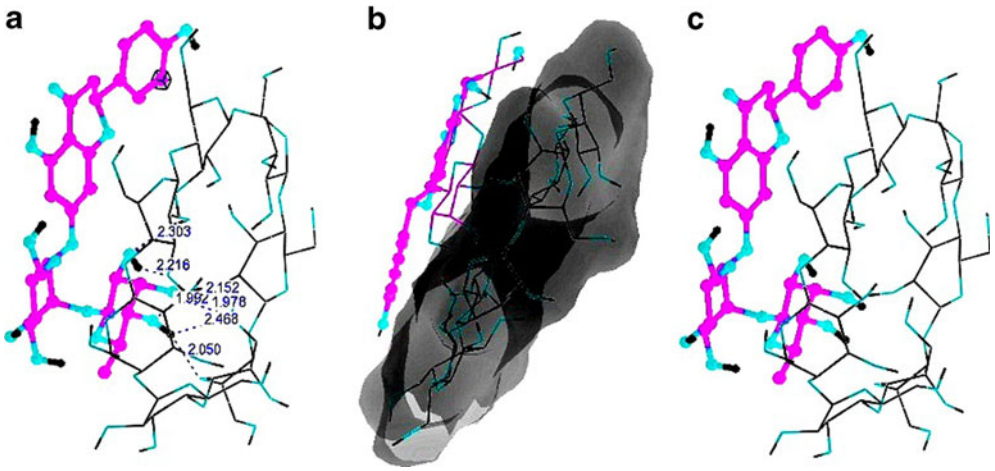

Fig. 5. Docking poses of naringin with β-cyclodextrin. **a** Hydrogen interaction. **b** Phobic interaction. **c** Electrostatic interaction

complex. The glide task most frequently performed is ligand docking (26). G-Score was found out to derive the strength of interactions (27).

RESULT AND DISCUSSION

Inclusion Complexation Between Nar and β-CD

Figure 1 shows the docking poses of Nar and β-CD (an assumed 1:1 interaction) binding with the glide score of −1.91. This shows the interaction of the possible group of Nar with β-CD theoretically. The existence of hydrogen bonding and phobic and electrostatic interaction can be seen. *In vitro* analysis was carried out to get further insight into the stoichiometry of the complex.

Considering UV–visible absorption spectra, two peaks (λ_{max}, 289 and 323 nm) can be noticed for the Nar (3.67×10^{-6} M) in the aqueous solution. These observed peaks such as high intensity and weak shoulder peak can be attributed to the presence of 5, 7-dihydroxy-2, 3-dihydro-4*H*-chromen-4-one and phenolic moiety present in the Nar structure. The addition of β-CD from 0 to 1×10^{-2} M to Nar results in the increase of absorbance at 289 nm (Fig. 2). It can be noticed that the increase in another shoulder peak which appeared at λ_{max}, 323 nm. It denotes the involvement of the two moieties such as 5, 7-dihydroxy-2, 3-dihydro-4*H*-chromen-4-one and phenol in the inclusion phenomenon on the addition of β-CD. The Benesi–Hildebrand plot (28) of $1/[A_s-A_o]$ *vs.* $1/[\beta\text{-CD}]^2$ for the formation of inclusion complex of Nar with β-CD is shown in the inset of Fig. 2. The binding constant between Nar and β-CD was calculated as 1.44×10^4 M^{-2} (correlation coefficient, 0.99). The linearity in the above plot shows the formation of 1:2 complexation between Nar and β-CD.

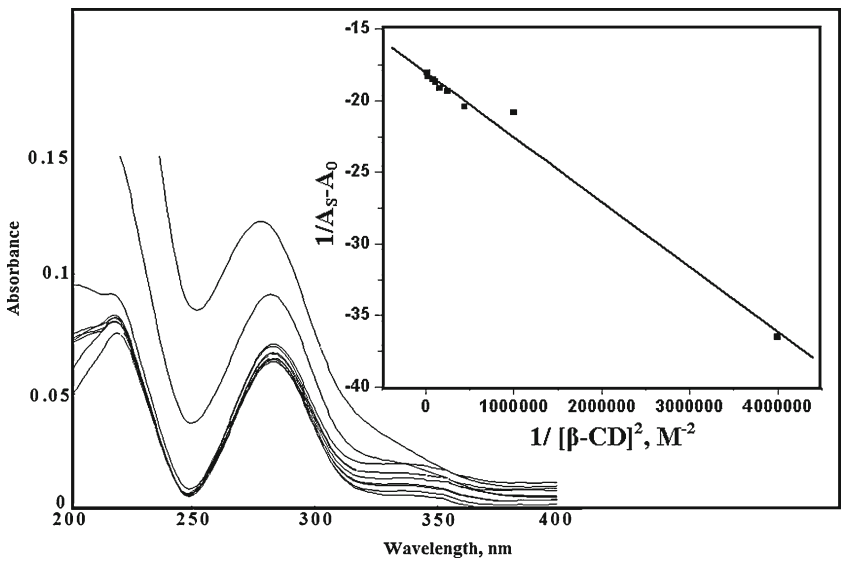

Fig. 6. Absorption spectra of naringin in the presence of various concentrations of β-cyclodextrin. *Inset* The plot of $1/A_s-A_0$ against $1/[\beta\text{-CD}]^2$ for the interaction of naringin in the presence of various concentrations of β-CD

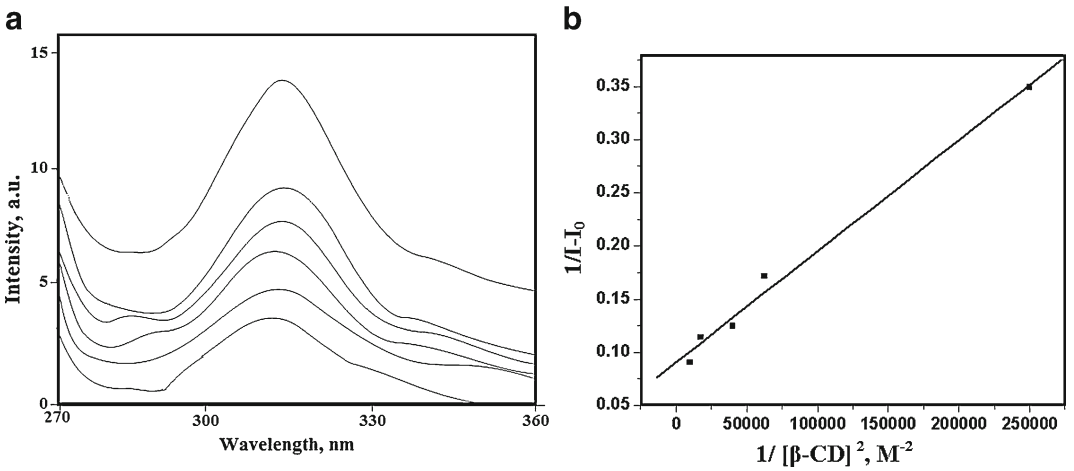

Fig. 7. **a** Fluorescence spectra of naringin in the presence of various concentrations of β-cyclodextrin. **b** The plot of $1/I-I_0$ against $1/[\beta\text{-CD}]^2$ for the interaction of naringin in the presence of various concentrations of β-CD

The inclusion complexation was further followed by the fluorescence spectral measurements. The fluorescence emission wavelength λ_{emi} at 323 and 368 nm was observed for the Nar in aqueous solution (Fig. 3a). Addition of β-CD from 0 to 1×10^{-2} M concentration resulted in fluorescence enhancement of both the fluorescence emission maxima. A slight blue shift of λ_{emi} from 368 nm was observed for the longer wavelength maximum. The above change might be the evidence for the inclusion complexation occurring between Nar and β-CD. The Benesi–Hildebrand equation for 1:2 binding is given by

$$\frac{1}{\mathrm{I}-\mathrm{I}_0}=\frac{1}{\mathrm{I}'-\mathrm{I}_0}+\frac{1}{\mathrm{I}'-\mathrm{I}_0}\,\frac{1}{K\,[\beta\text{-CD}]^2} \qquad (1)$$

where I_0, I, I′, and K are the intensities of fluorescence of the fluorophores without β-CD, intensity with varying concentrations of β-CD, intensity with the maximum concentration of β-CD, and the binding constant, respectively. The stoichiometry is found to be 1:2 for the inclusion complex (guest/host) with the binding constant of 6.53×10^4 M^{-2} (correlation coefficient, 0.99) (Fig. 3b). This observation of 1:2 complexation is in accordance with the results obtained by the absorption measurements.

It is well-known that the inner diameter and the height of β-CD moiety are 0.62–0.78 and 0.79 nm, respectively (29). The bond length of Nar, calculated by Rasmol Version 2.7.5.2, supports the possibility of inclusion complexation between and Nar and β-CD (Fig. 4). From the

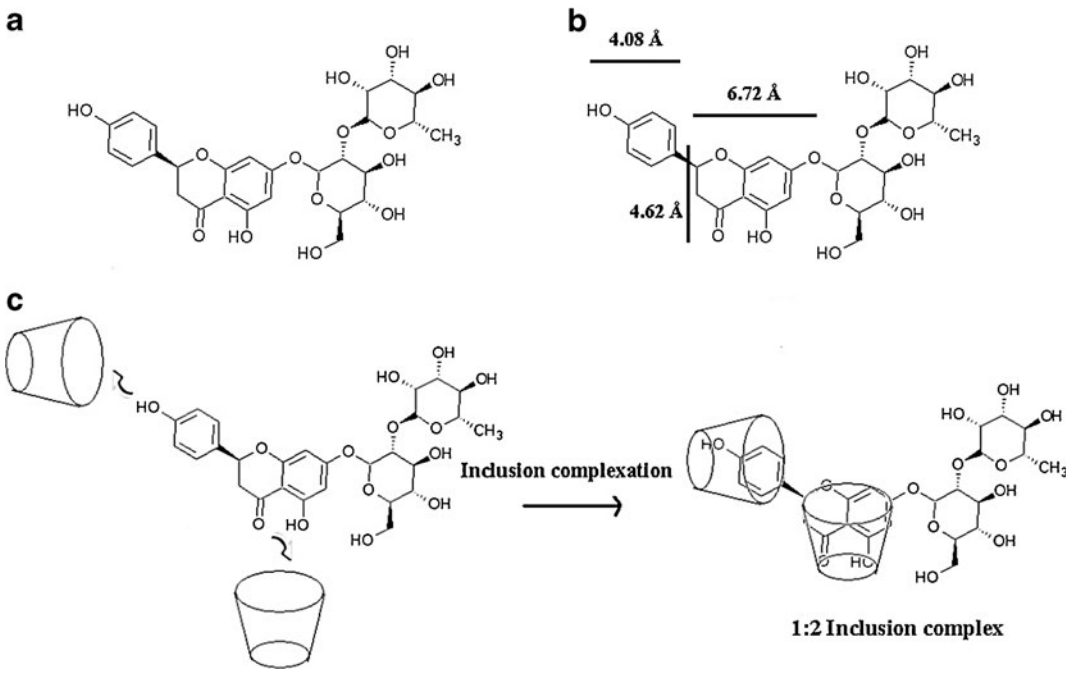

Fig. 8. **a** The molecular structure of naringin. **b** The calculated Length and width of naringin. **c** Schematic diagrams of the 1:2 inclusion complexation of naringin with β-CD

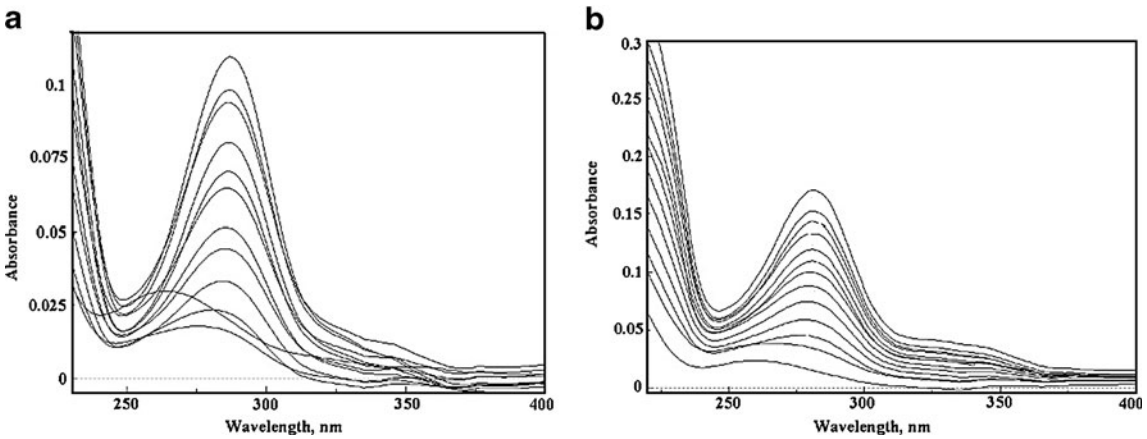

Fig. 9. **a** Absorption spectra of calf thymus DNA in the presence of various concentrations of naringenin. **b** Absorption spectra of calf thymus DNA in the presence of various concentrations of naringin

above discussion, the proposed model of the 1:2 complexes can be depicted as in Fig. 4.

Inclusion Complexation of Narn with β-CD

Figure 5 shows the docking poses on the interaction between Narn and β-CD (an assumed 1:1 interaction) with the glide score of −4.94. It confirms the possible strong interaction of Narn with β-CD rather than with Nar.

Two peaks can be noticed in the absorption spectra for the Narn (3.44×10^{-6}M) in the aqueous solution. These peaks (λ_{max}, 282 and at ≈326 nm) such as high intensity and weak a shoulder can be attributed to the presence of neohesperidoside linked 5, 7-dihydroxy-2, 3-dihydro-4*H*-chromen-4-one and phenolic moiety present in the structure. No considerable change in λ_{max} was observed for Narn by the addition of β-CD from 0 to 8×10^{-3} M from 282 (Fig. 6). The decrease in the absorbance was noticed with respect to the two peaks on the β-CD titration. It denotes the involvement of both the moieties with respect to β-CD addition leading to the formation of inclusion complexation of Narn. The Benesi–Hildebrand plot of $1/[A_s-A_0]$ *vs.* $1/[\beta\text{-CD}]^2$ for the formation of inclusion complex of Narn with β-CD is shown in the inset of Fig. 6. The calculated binding constant between Nar and β-CD was 39.78×10^5 M^{-2} (correlation coefficient, −0.99) (inset of Fig. 6). Thus, 1:2 stoichiometry was observed for the interaction of Narn and β-CD. This is in accordance with the strong glide score obtained for Narn–β-CD interaction than Nar–β-CD theoretically.

The inclusion complexation was further analyzed to confirm the binding and stoichiometry of the complex by the fluorescence spectral measurements. The fluorescence emission wavelength at 316 nm was observed for the Narn in aqueous solution (Fig. 7a). Addition of β-CD from 0 to 1×10^{-2} M concentration resulted in increase of the fluorescence intensity. The above observation might be due to the inclusion complexation of Narn with β-CD. The stoichiometry and the binding constant were determined from Benesi–Hildebrand

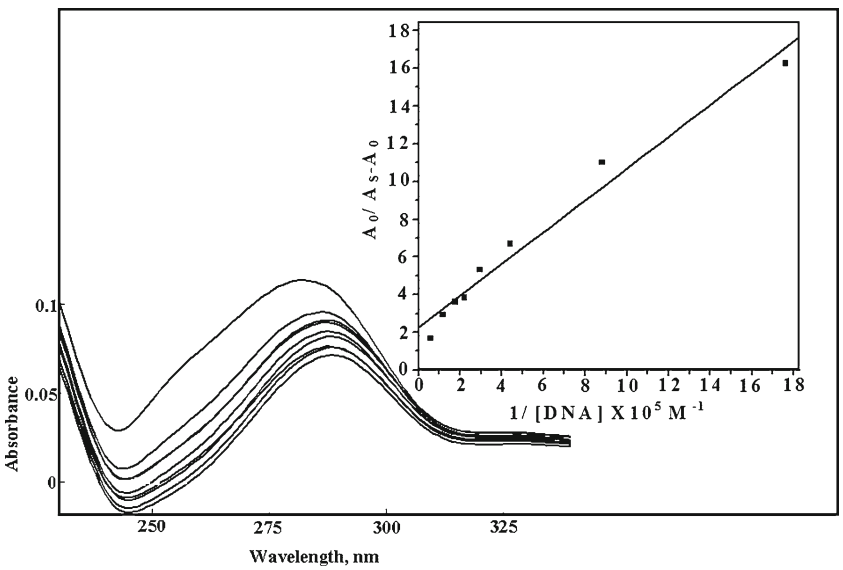

Fig. 10. Absorption spectra of naringenin in the presence of various concentrations of ctDNA. Inset The plot of A_0/A_s-A_0 against 1/[DNA] for the interaction of naringenin in the presence of various concentrations of ctDNA

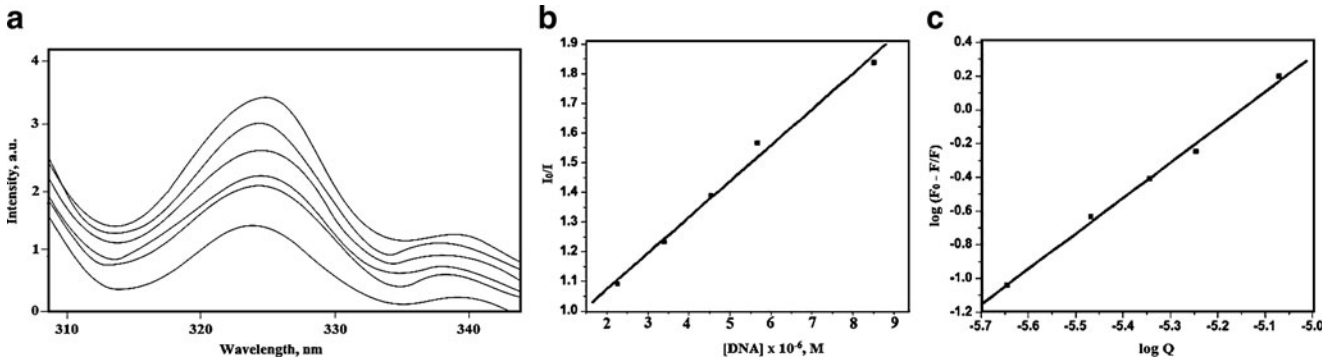

Fig. 11. **a** Fluorescence spectra of naringenin in the presence of various concentrations ctDNA. **b** The plot of I_0/I against [DNA] for the interaction of naringenin in the presence of various concentrations of ctDNA. **c** The plot of LogF_0–F/F against Log$Q$ for the interaction of naringenin in the presence of various concentrations of ctDNA

plot given in Eq. (1). The stoichiometry is found to be 1:2 for the inclusion complex (guest/host) with the binding constant of 8.68×10^4 M^{-2} given in Fig. 7b (correlation coefficient, 0.99).

The bond length of Narn calculated by the Rasmol Version 2.7.5.2 supports the idea of inclusion complexation between and Narn and β-CD (Fig. 8). From all the discussion, the proposed model of the 1:2 complexes can be proposed as in Fig. 8.

Interaction Between Nar and ctDNA

The addition of various concentrations of Nar (0 to 6×10^{-6} M) to ctDNA (5.67×10^{-6} M) resulted in a red shift of the absorption band of DNA which found at 260 nm (Fig. 9a). This shows the interaction of Nar with ctDNA. The effect of quencher (ctDNA) was analyzed by the addition of varying concentrations of ctDNA to Nar (3.67×10^{-6} M), which resulted in absorption spectral changes, i.e., λ_{max} from 288 to 282 nm up to a concentration of 1.70×10^{-5} M. The increase in the absorbance of λ_{max} 288 was noted, whereas the peak at λ_{max} 323 nm remains unaltered either in terms of absorbance or absorption maximum wavelength (Fig. 10). This might be due to the interaction of 5, 7-dihydroxy-2, 3-dihydro-4*H*-chromen-4-one moiety with the ctDNA. From the variation of absorbance, the binding constant K of Nar–ctDNA complex was obtained according to the following equation (30).

$$\frac{A_0}{\mathrm{A}-\mathrm{A}_0}=\frac{\varepsilon_G}{\varepsilon_{H-G}-\varepsilon_G}+\frac{\varepsilon_G}{\varepsilon_{H-G}-\varepsilon_G}\frac{1}{K[\mathrm{DNA}]} \qquad (2)$$

where A_0 and A are the absorbance of the free quest and the apparent one and ε_G and ε_{H-G} are their absorption coefficients, respectively. The plot of $A_0/A-A_0$ *vs.* 1/[DNA] following Eq. (2) is shown in the inset of Fig. 10. The binding constant for Nar–ctDNA binding is calculated as 2.68×10^5 M^{-1} (correlation coefficient, 0.98).

The interaction of Nar with ctDNA was studied with fluorescence spectroscopy (Fig. 11a). The concentration of Nar is kept fixed at 3.67×10^{-6} M, whereas ctDNA concentration is increased from 0 to 8.51×10^{-6} M in stepwise addition. Nar showed weak fluorescence (excitation wavelength, 288 nm). However, the presence of ctDNA resulted in fluorescent quenching which might be due to the interaction of Nar with ctDNA. The stoichiometry and their

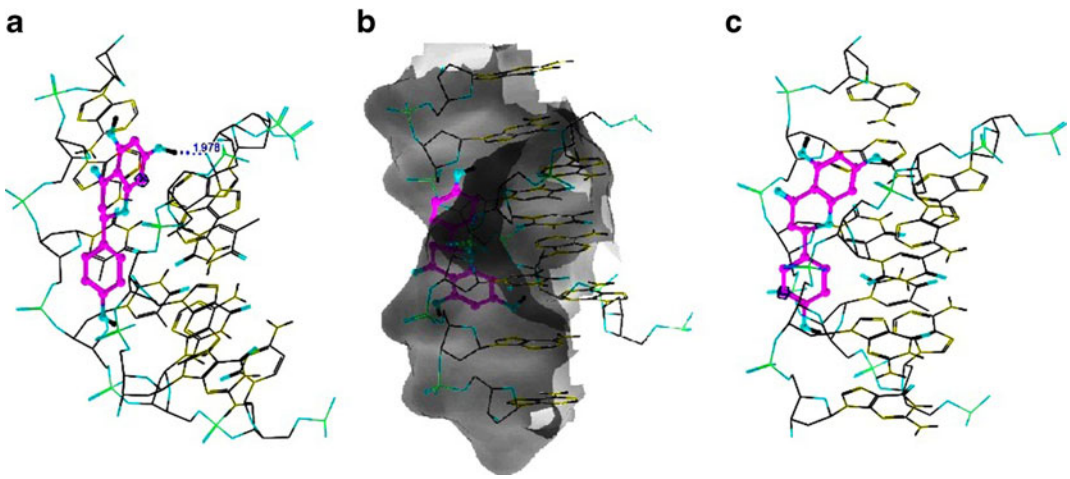

Fig. 12. Docking poses of naringenin with DNA. **a** Hydrogen interaction. **b** Phobic interaction. **c** Electrostatic interaction

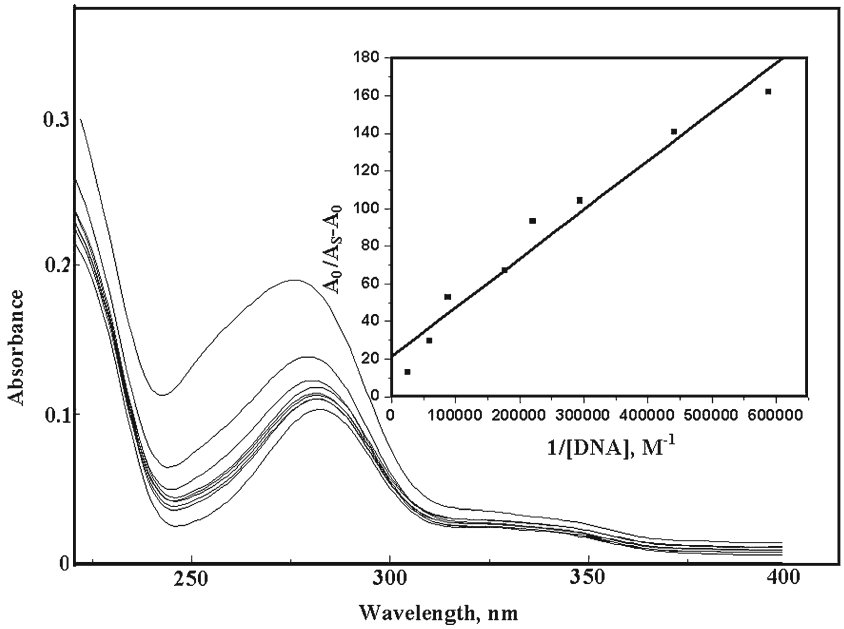

Fig. 13. Absorption spectra of naringin in the presence of various concentrations of ctDNA. Inset The plot of A_0/A_s-A_0 against 1/[DNA] for the interaction of naringin in the presence of various concentrations of ctDNA

association constant were determined from the fluorescence spectral data. The quenching constant between Nar and DNA was calculated as 1.21×10^5 M^{-1} (correlation coefficient, 0.99) (Fig. 11b) following Stern–Volmer equation (31) given by

$$\frac{F_0}{F} = 1 + K_{sv}[Q] \tag{3}$$

where F_0 and F are the fluorescence intensities in the absence and the presence of fluorophore respectively. $[Q]$ is the quencher concentration and K_{sv} is the Stern–Volmer quenching constant. The binding constant K_b and the number of binding sites n were determined by using the fluorescence spectral changes on titration with ctDNA (32).

$$\text{Log}\ (\frac{F_0}{F} - F) = \text{Log}K_b + n\text{Log}[Q] \tag{4}$$

The above equation was utilized for the plotting of double logarithm regression curve (Fig. 11c) of log (F_0-F/F) *versus* log $[Q]$. The binding constant K_b and the number of binding sites n for the interaction between Nar and ctDNA in the aqueous solution were determined from the plot. The number of binding sites n calculated for Nar and ctDNA is 2.10, i.e., approximately 2. This suggested the 1:2 stoichiometric interactions of Nar and ctDNA. The binding constant (K_b) of Nar binding with ctDNA was 6.68×10^{10} M^{-1} (correlation coefficient, 0.99). The interaction between Nar and DNA was further confirmed by docking studies. Figure 12 shows the docking model for the interaction between Nar and DNA. A distance of separation of 1.978 Å was observed for the interaction between oxygen of adenine moiety of the *B* strand of modeled DNA and hydrogen atom of Nar. The glide score observed was −5.37.

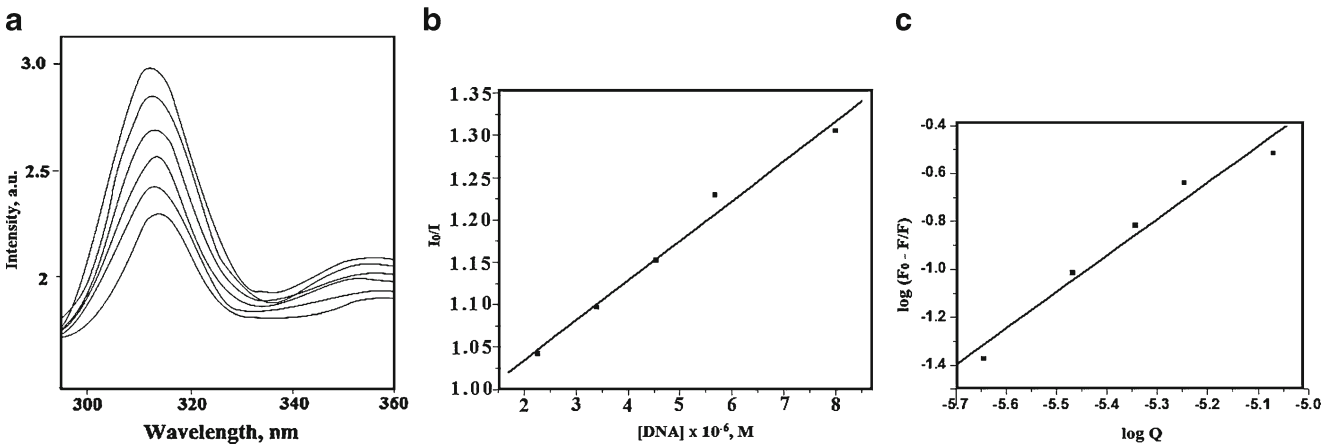

Fig. 14. **a** Fluorescence spectra of naringin in the presence of various concentrations ctDNA. **b** The plot of I_0/I against [DNA] for the interaction of naringin in the presence of various concentrations of ctDNA. **c** The plot of LogF_0-F/F against Log$Q$ for the interaction of naringin in the presence of various concentrations of ctDNA

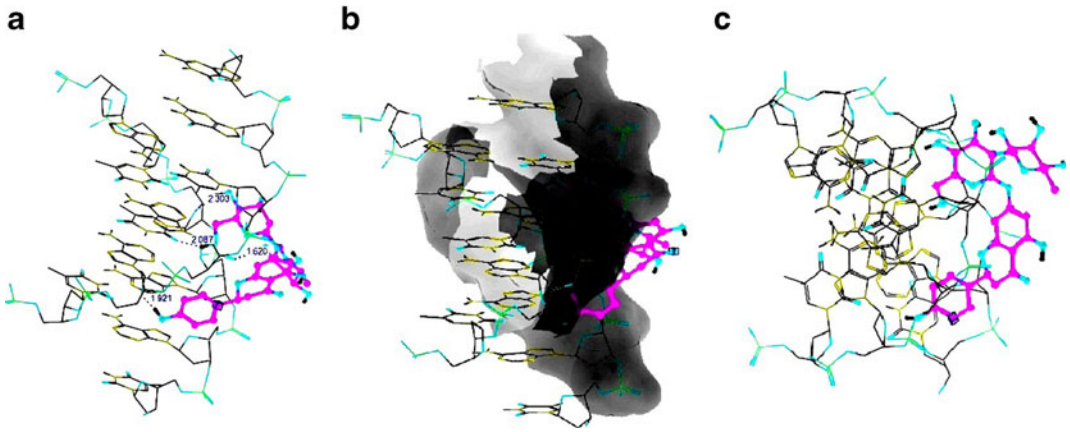

Fig. 15. Docking poses of naringin with DNA. **a** Hydrogen interaction. **b** Phobic interaction. **c** Electrostatic interaction

Interaction Between Narn and ctDNA

Addition of various concentrations of Narn (0 to 6×10^{-6} M) to ctDNA (5.67×10^{-6} M) resulted in red shift of the absorption band of DNA centered at 260 nm (Fig. 9b). Similarly, addition of varying concentrations of ctDNA resulted in absorption spectral changes of λ_{max} of Narn (3.96×10^{-6} M) from 282 to 276 nm up to the concentration of 4×10^{-5} M (Fig. 13). The absorbance increased on each addition. Based on the variation of absorbance, the binding constant K of Narn–ctDNA complex was obtained following Eq. (3). The plot of $A_0/A-A_0$ *vs.* 1/[DNA] is shown in the inset of Fig. 13. The binding constant for Narn–ctDNA binding was calculated as 8.22×10^4 M^{-1} (correlation coefficient, 0.97). It was further analyzed by fluorescence spectral results.

The interaction of Narn with ctDNA on titration up to 8×10^{-6} M was studied with steady-state fluorescence spectroscopy (Fig. 14a). Narn showed weak fluorescence at λ_{emi} 315 nm (excitation wavelength, 282 nm). Decrease in the fluorescence intensity was noticed with no significant shift in the emission maximum of Narn. The calculated quenching constant between Narn and ctDNA was 4.70×10^4 M^{-1} (correlation coefficient, 0.99) (Fig. 14b) following Stern–Volmer Eq. (3) (31).

The binding constant (K_b) and the number of binding sites n for the interaction between Narn and ctDNA in the aqueous solution were determined from Fig. 14c. The number of binding sites (n) calculated for Nar and ctDNA was 1.52 (approximately 1.5). This showed the 1:1.5 stoichiometric interactions of Narn and ctDNA. The binding constants K_b of Nar and with ctDNA was 1.89×10^7 M^{-1} (correlation coefficient, 0.98). This decrease might be due to the existence of steric effect caused by neohesperidoside moiety in Narn. Figure 15 shows the docking model for the interaction between Narn and DNA. The glide score observed was −6.48. The bond lengths observed for the interaction between DNA and Narn is given in Table I.

Table I. The Interactions and Bond Length Observed for the Binding Between DNA and Narn by Docking Techniques

Nucleotide	DNA strand	DNA atom	Ligand atom	Bond length
T6	A	O4	H	2.303
T6	A	O2	H	2.087
A7	A	O1P	O	1.620
A7	B	O4	O	1.921

The Influence of β-CD on Nar–ctDNA Binding

The titration of Nar–β-CD with DNA, by the addition of ctDNA from 0 to 4×10^{-5} M concentration, resulted in the shift of the absorption maximum from 287 to 272 nm (Fig. 16). The formation of isosbestic point at ~310 nm denotes the formation of new species on Nar–β-CD with the addition of ctDNA. Based on the variation of absorbance, the binding constant was obtained as 9.10×10^4 M^{-1} (correlation coefficient, 0.99) (inset of Fig. 16).

The titration of Nar–β-CD solution against ctDNA resulted in quenching of fluorescence without significant shift of emission wavelength maximum of Nar–β-CD found at λ_{emi} 323 nm in aqueous solution (Fig. 17a). The quenching constant K_{sv} calculated for the interaction of Nar and ctDNA in β-CD solution was 1.12×10^5 M^{-1} (correlation coefficient, 0.98) (Fig. 17b). This value is in accordance with the K_{sv} of Nar–ctDNA in aqueous solution. No significant change was observed in K_{sv} for Nar–ctDNA in the presence of β-CD. This show that the inclusion complexation occurred between Nar and β-CD does not disturb on the interaction with ctDNA. This observation shows the interaction of inclusion complex of Nar by including a portion of Nar thereby allowing the free interaction of the other free exposed moiety with ctDNA. On other hand, it can be explained in detail as follows. From the inclusion studies of Nar and β-CD, it can be seen that the phenolic and dihydrochromene prefers to interact with beta CD thereby forming 1:2 complexation. Fluorescence quenching phenomenon was observed for Nar and ctDNA binding. It can be seen that dihydrochromene prefers to bind with DNA. Similarly, fluorescence quenching phenomenon

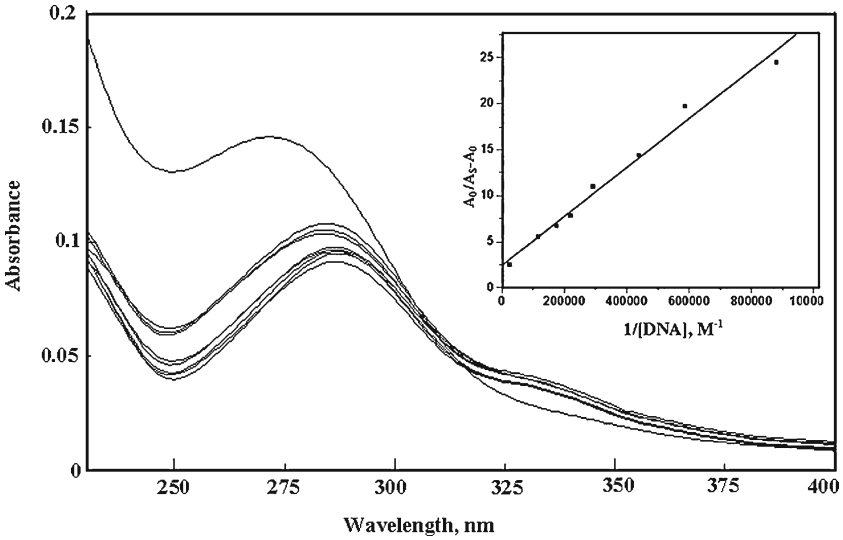

Fig. 16. Absorption spectra of naringenin–β-CD complex in the presence of various concentrations of ctDNA. *Inset*: The plot of A_0/A_s-A_0 against 1/[DNA] for the interaction of naringenin–β-CD complex in the presence of various concentrations of ctDNA

was observed for Nar–β-CD on the addition of ctDNA. This shows the extraction of Nar preferably dihydrochromene moiety from the cavity of beta CD for the binding with DNA. Further evidence for this suggestion could be the binding constant K_b and binding sites n viz., 2.51×10^5 M^{-1} and 1.07, respectively (correlation coefficient, 0.94) (Fig. 17c). Two portions viz., phenolic and dihydrochromene moieties, are proposed interacting with two DNA molecules separately in the absence of β-CD solution. In the presence of β-CD, the inclusion complex of Nar might prefer to interact with DNA by interacting through one of its moiety thereby reducing the original number of binding sites from 2 to 1.

The Influence of β-CD on Narn–ctDNA Binding

The addition of ctDNA from 0 to 4×10^{-5} M to the Narn–β-CD solution resulted in the shift of absorption maximum from 283 to 272 nm (Fig. 18). The binding constant K of Narn–ctDNA complex in the presence of β-CD was 4.90×10^4 M^{-1} (correlation coefficient, 0.98) according to Eq. (2).

The addition of ctDNA resulted in the fluorescence quenching of Narn–β-CD complex without the considerable shift of emission maximum of Narn found at λ_{emi} 316 nm (Fig. 19). The calculated quenching constant K_{sv} was 8.54×10^3 M^{-1} (correlation coefficient, 0.98). However, the binding constant K_b and the number of sites n determined were 5.88 M^{-1} and 0.32 (approximately 0.3) (correlation coefficient, 0.95). The strong hydrogen bonding interaction between β-CD and the moiety, neohesperidoside of Narn, might have resulted in the smaller quenching constant value of Narn–ctDNA in the presence of β-CD comparing to Nar–ctDNA in the β-CD solution. The binding site n also reduced to 0.3 for Narn–ctDNA in presence of β-CD solution. This observation

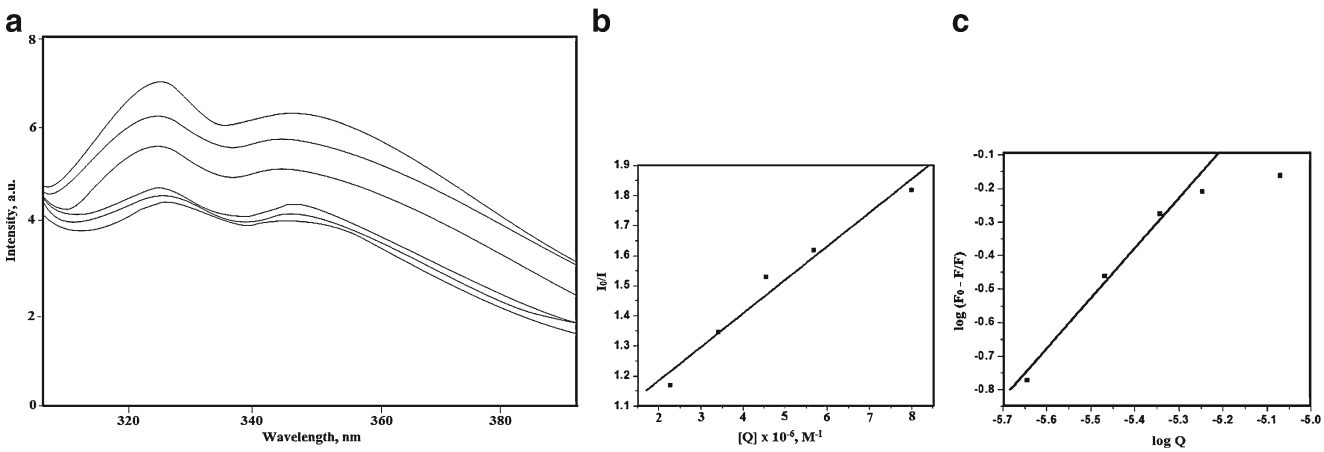

Fig. 17. **a** Fluorescence spectra of naringenin–β-CD complex in the presence of various concentrations ctDNA. **b** The plot of I_0/I against [DNA] for the interaction of naringenin–β-CD complex in the presence of various concentrations of ctDNA. **c** The plot of LogF_0-F/F against Log$Q$ for the interaction of naringenin–β-CD complex in the presence of various concentrations of ctDNA

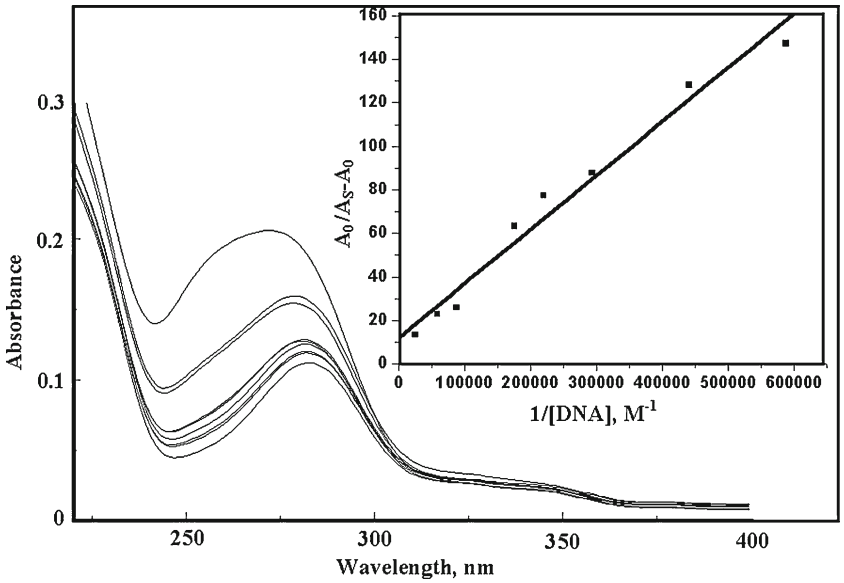

Fig. 18. Absorption spectra of naringin–β-CD complex in the presence of various concentrations of ctDNA. *Inset*: The plot of A_0/A_s-A_0 against 1/[DNA] for the interaction of naringin–β-CD complex in the presence of various concentrations of ctDNA

was also different from the observed higher interaction of Narn and ctDNA in aqueous solution. This might be due to the extraction of the bound drug from DNA by formation of inclusion complex with β-CD. The inclusion complex formed between Narn and β-CD does not have much preference to get interacted with ctDNA for the tri-component complex formation.

CONCLUSION

Nar and Narn form 1:2 stoichiometric inclusion complexes with β-CD. The binding sites *n* was determined as 2 and 1 for the binding of Nar with ctDNA in aqueous solution and β-CD medium. The binding sites *n* was determined as 1.5 and 0.3 for the binding of Narn with ctDNA in aqueous solution and β-CD medium. Narn shows less significant interaction (n=0.3) with ctDNA in β-CD solution. This might be due to the extraction of the bound drug from DNA by formation of inclusion complex with β-CD. The neohesperidoside moiety present in Narn is involved with the stronger hydrogen bonding interaction with β-CD thereby preventing the availability of Narn to ctDNA. The binding constant (K_b=5.88 M^{-1}) for the interaction of Narn–β-CD with ctDNA is not significant, which shows that the inclusion complex of Narn does not have much preference for the interaction with DNA than that of Nar. The binding study of Nar and Narn in aqueous and Beta CD solution may act as ground work for the clinical use since the metabolism of naringin into naringenin is a key factor in humans.

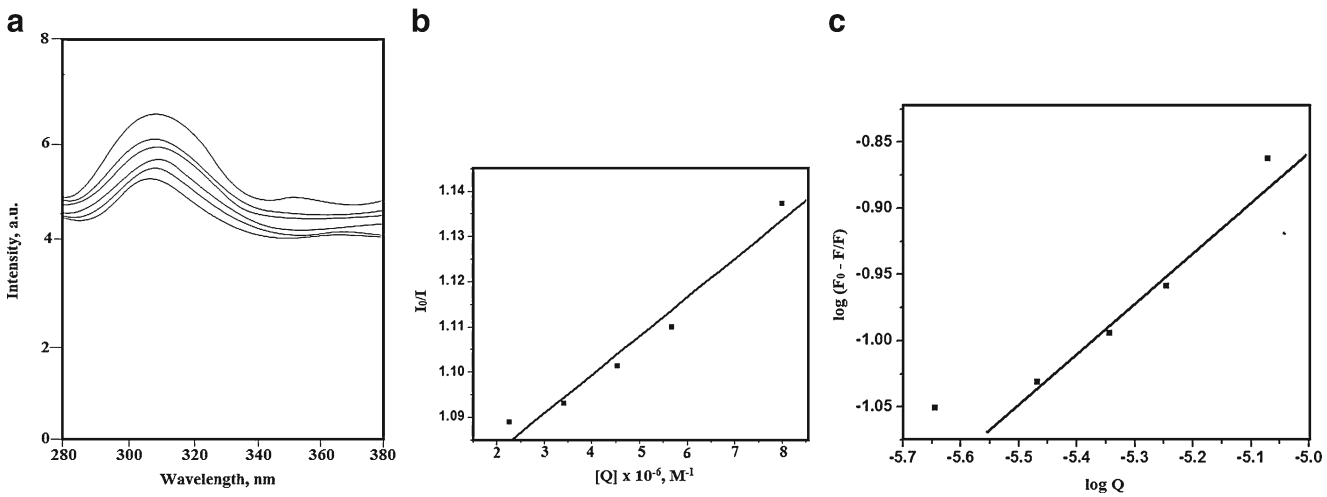

Fig. 19. **a** Fluorescence spectra of naringin–β-CD complex in the presence of various concentrations ctDNA. **b** The plot of I_0/I against [DNA] for the interaction of naringin–β-CD complex in the presence of various concentrations of ctDNA. **c** The plot of LogF_0-F/F against Log$Q$ for the interaction of naringin–β-CD complex in the presence of various concentrations of ctDNA

ACKNOWLEDGMENTS

This work is financially supported by the Department of Science and Technology (DST), Government of India (Project file: SR/FT/CS-062/2009) under Fast Tack Scheme for Young Scientists (SERB). We sincerely thank DST.

REFERENCES

1. Gong-Jun Y, Jing-Juan X, Hong-Yuan C, Zong-Zhou L. Studies on the interaction between rutin and DNA in the absence and presence of β-cyclodextrin by electrochemical and spectroscopic methods. Chin J Chem. 2004;22:1325–9.
2. Jonathan BC. Drug–DNA interactions. Curr Opin Struct Biol. 1998; 8(3):314–320.
3. Wang Q, Yang ZY, Qi GF, Qin DD. Crystal structures, DNA-binding studies and antioxidant activities of the Ln(III) complexes with 7-methoxychromone-3-carbaldehyde-isonicotinoyl hydrazone. Biometals. 2009;22:927–40.
4. Li Y, Yang ZY, Wang MF. Synthesis, characterization, DNA binding properties, fluorescence studies and antioxidant activity of transition metal complexes with hesperetin-2-hydroxy benzoyl hydrazone. J Fluoresc. 2010;20:891–905.
5. Tong C, Hu Z, Wu J. Interaction between methylene blue and calf thymus deoxyribonucleic acid by spectroscopic technologies. J Fluoresc. 2010;20:261–7.
6. Lui C, Cady NC, Batt CA. Nucleic acid-based detection of bacterial pathogens using integrated micro fluidic platform systems-review. Sensors. 2009;9:3713–44.
7. Kalpana R, Cristol SM, Mehta M, Nickerson JM. Quantifying DNA concentrations using fluorometry: a comparison of fluorophores. Mol Vis. 2002;8:416–21.
8. Dean Farmer Jr J, Gustafson GR, Conti A, Zimmt MB, Suggs JW. DNA binding properties of a new class of linked anthramycin analogs. Nucleic Acids Res. 1991;19(4):899–903.
9. Dinesh kumar B, Vignesh Kumar P, Bhuvaneshwaran SP, Mitra A, Advanced drug designing softwares and their applications in medical research, Int J Pharm Pharmaceut Sci, 2010, 2(3):16–18.
10. Gattuso G, Barreca D, Gargiulli C, Leuzzi U, Caristi C. Flavonoid composition of citrus juices—review. Molecules. 2007;12:1641–73.
11. Jaganath IB, Crozier A. In: Cesar G. Fraga, editor. Dietary flavonoids and phenolic compounds, plant phenolics and human health: biochemistry, nutrition, and pharmacology. New York: Wiley; 2010. p. 1–49.
12. Gorinstei S, Huang D, Leontowicz H, Leontowicz M, Yamamoto K, Fortuny RS, *et al.* Determination of naringin and hesperidin in citrus fruit by high performance liquid chromatography. The antioxidant potential of citrus fruit. Acta Chromatogr. 2006;17:108–24.
13. Petersona JJ, Beecherb GR, Bhagwatc SA, Dwyera JT, Gebhardtc SE, Haytowitzc DB, *et al.* Flavanones in grapefruit, lemons, and limes: a compilation and review of the data from the analytical literature—critical review. J Food Compos Anal. 2006;19:S74–80.
14. Gorinstein S, Leontowicz H, Leontowicz M, Krzeminski R, Gralak M, Jastrzebski Z, *et al.* Effect of hesperidin and naringin on the plasma lipid profile and plasma antioxidant activity in rats fed a cholesterol-containing diet. J Sci Food Agric. 2007;87:1257–62.
15. Ajay S, Mona S, Singh D, Rawat MSM. Preparation and characterization of phospholipid complexes of naringenin for effective drug delivery. J Incl Phenom Macrocycl Chem. 2010;67:253–60.
16. Cho KW, Kim YO, Andrade JE, Burgess JR, Kim YC. Dietary naringenin increases hepatic peroxisome proliferators-activated receptor a protein expression and decreases plasma triglyceride and adiposity in rats. Eur J Nutr. 2011;50:81–8.
17. Liu M, Zou W, Yang C, Peng W, Su W. Metabolism and excretion studies of oral administered naringin, a putative antitussive, in rats and dogs. Biopharmaceutics and Drug disposition. 2012;33(3):123–34.
18. Fuhr U, Kummert AL. The fate of naringin in humans: a key to grapefruit juice-drug interactions? Clin Pharmacol Ther. 1995;58:365–73.
19. Piamsook P, Bruce MA. Interactions of methyl-beta-cyclodextrin with adenine and pyridine/nicotinamide derivatives as determined by competitive fluorescence methods. J Sci Soc Thailand. 1998;24:37–44.
20. French D. Adv Carbohydr Chem. 1957;12:189–260.
21. Thorsteinn LX, Brewster ME. Pharmaceutical applications of cyclodextrins. 1. Drug solubilization and stabilization—review article. J Pharm Sci. 1996;85:10.
22. Thorsteinn L, Pekka J, Mar M, Jomi J, Cyclodextrins in drug delivery. Expert Opin Drug Deliv. 2005; 2:335–51.
23. Sameena Y, Radhika D, Enoch IVMV, Murugesh E. The influence of β-cyclodextrin encapsulation on the binding of 2′-hydroxyflavanone with calf thymus DNA. Spectrochimica Acta A: Mol. Biomol. Spec. 2012; 98:405–12.
24. Schrodinger. Glide: a complete solution for ligand receptor docking [computer software]. Glide, version 5.5. New York: Schrödinger; 2009.
25. Lu Y, Wang GK, Lv J, Zhang GS, Liu QF. Study on the interaction of an anthracycline disaccharide with DNA by spectroscopic techniques and molecular modeling. J Fluoresc. 2011;21:409–14.
26. Glide: Schroedinger, Portland, OR. http://www.schrodinger.com.
27. Sameena Y, Sudha N, Murugesan G, Enoch IVMV. Isolation of prunin from the fruit shell of *Bixa orellana* and the effect of β-cyclodextrin on its binding with calf thymus DNA. Carbohydr Res. 2013; 365:46–51.
28. Huoa D, Yanga L, Houa C, Fad H, Luoa X, Lue Y, *et al.* Molecular interactions of monosulfonate tetraphenylporphyrin (TPPS1) and meso-tetra(4-sulfonatophenyl)porphyrin (TPPS) with dimethyl methylphosphonate (DMMP). Spectrochim Acta A. 2009;74:336–43.
29. Enoch IVMV, Swaminathan M. Stoichiometrically different inclusion complexes of 2-aminofluorene and 2-amino-9-hydroxyfluorene in β-cyclodextrin: a spectrofluorimetric study. J Fluoresc. 2006;16:697–704.
30. Ensafi AA, Hajian R, Ebrahimi S. Study on the interaction between morin-Bi (III) complex and DNA with the use of methylene blue dye as a fluorophor probe. J Braz Chem Soc. 2009;20:266–76.
31. Lakowicz JR. Principles of fluorescence spectroscopy. New York: Plenum; 1999.
32. Bakkialakshmi S, Chandrakala D. Fluorometric investigation on the interaction of 5-bromo and 5-iodouracil with bovine serum albumin. Archives of Applied Science Research. 2011;3(2):174–9.